Journal of Nano- and Electronic Physics
Vol. **18** No 1, 01033(5pp) (2026)

Журнал нано- та електронної фізики
Том **18** № 1, 01033(5cc) (2026)

OPEN ACCESS

REGULAR ARTICLE

A Decagonal Quad-Band Slitted Microstrip Antenna for 5G Wireless Networks

Faez M.B. Abdo[1,*], Abdul Guddoos S.A. Gaid[1,†], Mohammad Ahmed Alomari[2], Imran Mohd Ibrahim[3], Mukhtar Ghaleb[4]

[1] *Faculty of Engineering & Information Technology, Taiz University, Taiz, Yemen*
[2] *Faculty of Artificial Intelligence and Cyber Security (FAIX), Universiti Teknikal Malaysia Melaka (UTeM), Melaka, Malaysia*
[3] *Centre for Telecommunication Research and Innovation (CeTRI), Fakulti Teknologi Kejuruteraan Elektronik dan Komputer, Universiti Teknikal Malaysia Melaka (UTeM), Melaka, Malaysia*
[4] *College of Computing and Information Technology, University of Bisha, 67714 Bisha, Saudi Arabia*

(Received 05 January 2026; revised manuscript received 20 February 2026; published online 25 February 2026)

With the rapid advancement of 5G wireless networks, there is a growing need for compact, high-performance antennas capable of operating across multiple mm-Wave bands. Microstrip patch antennas are ideal for 5G handsets due to their low profile and ease of integration. However, achieving high gain, wide bandwidth, and efficiency in a compact form remains challenging. This paper presents a decagonal quad-band microstrip antenna designed for operation at 28, 38, 45, and 60 GHz. The antenna, constructed on an Arlon AD 255C substrate ($12 \times 12 \times 0.66$ mm^3), incorporates three slits to enhance impedance matching and radiation performance. Simulated results show bandwidths of 1.6, 2.5, 5, and 15 GHz with peak gains of 5.9, 7.8, 7.5, and 7.4 dBi, and efficiency ranging from 81.7 % to 93.5 %. The proposed antenna offers compact size, high gain, and multiband operation, making it a strong candidate for integration into next-generation 5G mobile devices.

Keywords: Quad-band, Slitted microstrip antenna, Compact antenna, Wireless networks, 5G.

DOI: 10.21272/jnep.18(1).01033 PACS number: 84.40.Ba

1. INTRODUCTION

5G technology enables very high data rates and low latency by operating in both sub-6 GHz and millimeter-wave (mm-Wave) bands. The sub-6 GHz spectrum is already heavily occupied, limiting its capacity [1]. In contrast, mm-Wave bands offer significantly wider bandwidths, making them key enablers of next-generation 5G systems. Regulatory bodies such as the WRCC, ITU, and FCC have identified mm-Wave bands between 24-86 GHz for 5G, with particular focus on 28, 38, 60, and 73 GHz, and the FCC allocating 57-64 GHz for unlicensed use. Additional unlicensed bands at 70/80, 90, and 164-200 GHz have also been proposed for future applications [2, 3]. Among these, the 28 and 38 GHz bands are especially promising for high-speed, low-latency communication [4, 5]. However, mm-Wave signals suffer from severe path loss, atmospheric absorption, and attenuation, necessitating the use of high-gain antennas [6, 7].

Various antenna architectures have been investigated to address these challenges. While aperture antennas provide high directivity, microstrip patch antennas are widely preferred for mm-Wave systems due to their compact size, low cost, and ease of integration with planar circuits [8]. Nevertheless, single-element patch antennas typically exhibit low gain (< 5 dBi), which is insufficient for most 5G applications [8]. Gain enhancement techniques such as slotting, slitting, and electromagnetic bandgap (EBG) structures have therefore been explored [9, 10]. Additionally, the growing demand for compact multiband antennas has motivated designs capable of operating across multiple mm-Wave bands within a single radiator.

Numerous multiband antennas for 5G have been reported. Tiwari et al. [11] proposed a dual-band 28/38 GHz rectangular patch with circular slots, achieving gains of 6.11/7.15 dBi and 1.54 GHz bandwidth. Sharaf et al. [6] presented a dual-patch design operating at 38/60 GHz with 6.5/5.5 dBi gain and 5.2 GHz bandwidth. Other notable designs include umbrella-shaped patches [12], slotted rectangular patches [8], integrated multi-patch structures [13], concentric and monopole-based radiators [14, 15], octagonal and elliptical antennas [16, 17], and slot-optimized designs using genetic algorithms [18, 19]. While several works [20-22] demonstrate multiband operation, most are limited to dual or triple-band performance with moderate gain.

Despite these advances, achieving high gain, compact size, multiband operation, and design simplicity simultaneously remains challenging. This work addresses this gap by presenting a compact quad-band single-element microstrip antenna. The suggested single-

* Correspondence e-mail: faeez.abdo.std@taiz.edu.ye
† quddoos.gaid@taiz.edu.ye

Cite this article as: F.M.B. Abdo et al., *J. Nano- Electron. Phys.* 18 No 1, 01033 (2026) https://doi.org/10.21272/jnep.18(1).01033

element antenna employs a decagonal patch with three rectangular slits to further enhance impedance matching and radiation performance.

The main contributions of this work are:
- **Quad-band operation:** Coverage of 28, 38, 45, and 60 GHz using three rectangular slits to improve return loss, gain, and radiation efficiency.
- **Compact design:** The designed antenna feature small footprints suitable for space-constrained 5G devices.

The remainder of this paper is organized as follows: Section 2 describes the antenna design; Section 3 presents the parametric study, and Section 4 provides the results of the optimized antenna while Section 5 concludes the paper.

2. THE ANTENNA DEVELOPMENT

This subsection presents the design and optimization of a slitted decagonal quad-band microstrip patch antenna for 5G applications. The design shown in Fig. 1 is built on an Arlon AD255C substrate (ε_r = 2.6, tanδ = 0.0014, thickness = 0.66 mm). The decagonal copper patch (0.035 mm thick) is printed on the top layer, while a full copper ground plane of the same thickness is placed on the bottom.

A five-stage iterative optimization using CST was employed to excite four resonant modes and tune them to the desired frequencies. In stage 1, a basic circular patch was used, yielding weak resonances except near 51 GHz and between 57-69 GHz as shown in Fig. 2, necessitating further refinement. In stage 2, the circular patch was trimmed into a decagon (r_p = 3.7 mm), producing resonances at 33.15, 42.2, 51.4, and 63.95 GHz with improved reflection coefficients and bandwidths (Fig. 2).

In stage 3, a rectangular slit (0.6 mm wide) was etched at an angle θ_1 = 23°, shifting the resonances to 28.6, 38.7, 52.2, and 63.3 GHz and significantly enhancing impedance matching. Stage 4 introduced a second angled slit (θ_2 = − 83°), resulting in resonances at 27.2, 40.35, 45.35, and 59.05 GHz, with wide combined bandwidth coverage across the 38-47.7 GHz range and over 10 GHz at 60 GHz.

Finally, in stage 5, a third slit was added on the lower-left side (θ_3 = 182°), yielding optimized resonances at 28, 37.8, 44.8, and 61.3 GHz with reflection coefficients below − 14 dB and bandwidths of 1.6, 2.5, 5, and 15 GHz, respectively as presented in Fig. 2.

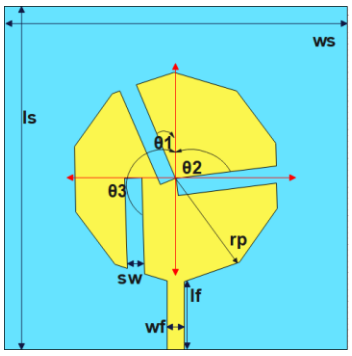

Fig. 1 – Geometry of the proposed antenna

The optimized basic decagonal antenna, shown in Fig. 1, is compact, measuring 12 × 12 × 0.66 mm^3. It is fed by a microstrip line with a length, l_f = 2.5 mm, and a width, w_f = 0.6 mm.

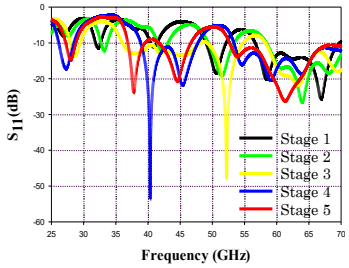

Fig. 2 – Simulated reflection coefficient performance across the five design stages

3. STUDY OF ANTENNA PARAMETERS

This section examines how several key antenna parameters influence the reflection coefficient (S_{11}), which indicates the antenna's operating frequency bands and the effectiveness of its impedance matching with the power feed line. The parameters studied include the slit width (s_w), the height of the dielectric substrate (h_s), and the slits' rotation angles (θ_1, θ_2, θ_3).

3.1 Varying the Slit Width (s_w)

Fig. 3 illustrates the impact of slit width (s_w) on the antenna's S_{11} response. The optimal slit width is 0.6 mm, balancing return loss and impedance bandwidth by tuning resonant modes through controlled current perturbation. Increasing s_w beyond 0.6 mm disrupts the current distribution, detuning and narrowing the bandwidth of the 60 GHz band. Conversely, reducing s_w below 0.6 mm weakens perturbation, improving matching at 28 but harming performance at 38, 45, and 60 GHz due to insufficient mode excitation. This highlights the importance of slit width for stable multiband performance.

3.2 Varying Height of the Dielectric Substrate (h_s)

Fig. 4 depicts the impact of substrate thickness (h_s) on the antenna's S_{11} response. The optimal thickness of 0.66 mm produces four resonant bands at 28, 37.8, 44.8, and 61.3 GHz, with reflection coefficients of – 14.7, – 23.8, – 20.7, and – 26.3 dB and bandwidths of 1.6, 2.5, 5, and 15 GHz, respectively. Reducing hs by 0.2 mm adds an additional resonance, resulting in bands at 27.2, 37.5, 43, 56.75, and 63.3 GHz, with S_{11} values of – 18.4 to – 28.7 dB and varying bandwidths indicating increased modal merging. Conversely, increasing h_s by 0.2 mm causes band splitting, leading to five main resonances, with reflection coefficients ranging from – 11.7 dB at 28.85 GHz to – 29 dB at 62.55 GHz and various bandwidths. These findings underscore the importance of substrate thickness in resonance behavior, bandwidth, and impedance matching.

3.3 Varying the Slits' Rotation Angles

This subsection explores how the rotation angles of slits (θ_1, θ_2, and θ_3) affect the antenna's S_{11} performance,

impacting resonance behavior, impedance matching, return loss, and additional band formation. The optimal angles are $\theta_1 = 23°$, $\theta_2 = -83°$, and $\theta_3 = 182°$, resulting in the best impedance matching and lowest return loss. Fig. 5 shows that reducing θ_1 from 23° to 0° improves matching at 28 GHz and 38 GHz with shifting the resonant frequencies. It also illustrates that setting θ_2 to zero with $\theta_1 = 23°$ and $\theta_3 = 182°$ leads to the emergence of unwanted resonant bands, while some desired bands may disappear. Additionally, changing θ_3 to zero while keeping θ_1 and θ_2 fixed degrades the reflection coefficient and shifts resonance frequencies.

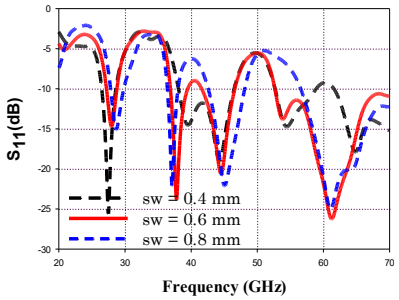

Fig. 3 – Reflection coefficient performance for different slit widths

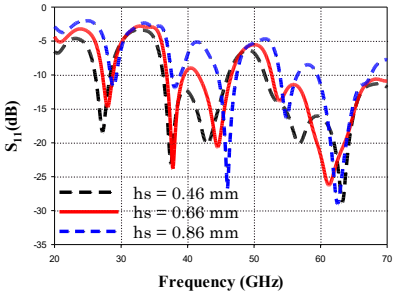

Fig. 4 – Reflection coefficient for different substrate heights

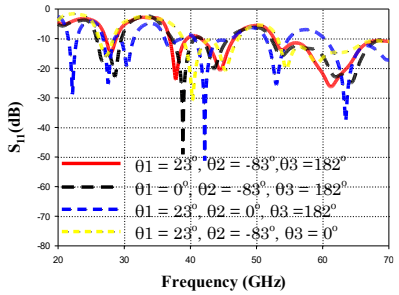

Fig. 5 – Reflection Coefficient for different rotation angles

4. DESIGN ASSESSMENT

The antenna was optimized in CST Studio Suite and validated using ANSYS HFSS. High consistency between these platforms confirms the design's robustness and ensures performance accuracy across the operating bandwidth, thereby minimizing fabrication risks. The following subsections examine and validate the primary antenna characteristics.

4.1 The Reflection Coefficient Performance

Fig. 6 compares the reflection coefficient (S_{11}) of the proposed antenna obtained from CST, and HFSS. CST results show four resonances at 28, 37.8, 44.8, and 61.3 GHz with reflection coefficients of – 14.7, – 23.8, – 20.7, and – 26.3 dB, and bandwidths of 1.6, 2.5, 5, and 15 GHz, respectively. HFSS simulations exhibit closely matching resonances at 28, 38, 44.8, and 64.5 GHz, with S_{11} values of – 13.02, – 25.9, – 23.1, and – 25.2 dB, and bandwidths of 1.23 GHz, 9.8 GHz (37.2 GHz to 47 GHz), and approximately 15 GHz. further validating the design. Overall, CST and HFSS results show strong correlation, with minor deviations attributed to differences in meshing and numerical solvers.

4.2 The VSWR

Fig. 7 compares the VSWR responses obtained from CST and HFSS simulations. CST yields VSWR values of 1.4495, 1.1374, 1.2285, and 1.1025 at 28, 37.8, 44.8, and 61.3 GHz, respectively, while HFSS shows VSWR values of 1.5760, 1.2817, 1.1509, and 1.2893. Both results indicate excellent impedance matching with minimal reflection across all bands. Moreover, the bandwidths meeting the VSWR ≤ 2 criterion closely match those obtained from $S_{11} \leq -10$ dB, confirming strong agreement between the two solvers and validating the design accuracy.

4.3 Far Field Radiation Characteristics

Fig. 8 compares the 2D radiation patterns from CST and HFSS simulations. Both show directional far-field patterns. CST peak gains are 5.9, 7.8, 7.5, and 7.4 dBi, at the resonances, with E-plane beamwidths of 54.4°, 48°, 44.9°, and 60.8° and H-plane beamwidths of 122.1°, 97.3°, 50.7°, and 48.3°. HFSS shows gains of 8, 8.8, 8.1, and 7.3 dBi, with *E*-plane beamwidths of 52°, 50°, 48°, and 48° and *H*-plane beamwidths of 96°, 112°, 58°, and 56°. Despite minor differences, both simulations confirm consistent directional behavior. Fig. 9 shows the gain and radiation efficiency across the frequency bands. Gain ranges from 5.8 dBi at 27.5 GHz to 8.7 dBi at 55 GHz, while radiation efficiency ranges from 81.7 % up to 93.5 %. The radiation characteristics are in good agreement, validating the antenna design and performance.

4.4 Surface Current Distribution

Fig. 10 shows the surface-current distributions at the resonant frequencies 28, 37.8, 44.8, and 61.3 GHz. The currents concentrate along the feed, the inner slits' edges, and circulate around the radiator outer edges.

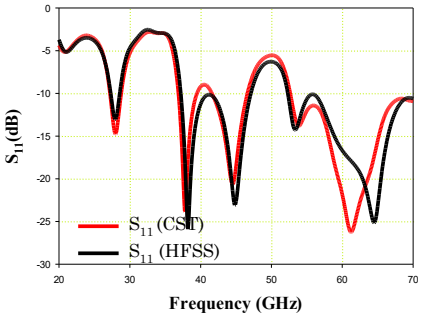

Fig. 6 – Reflection coefficient performance of the proposed antenna using CST, HFSS

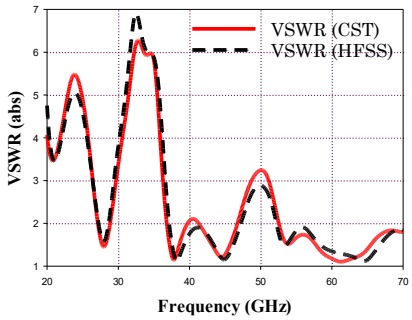

Fig. 7 – VSWR of the proposed antenna using CST and HFSS

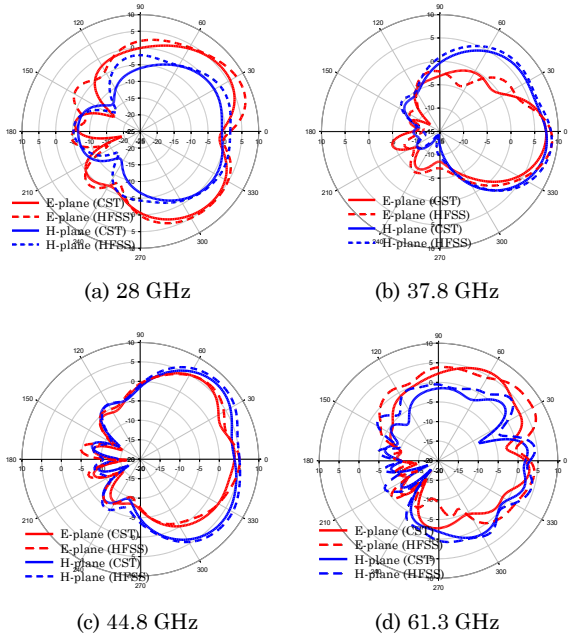

(a) 28 GHz (b) 37.8 GHz

(c) 44.8 GHz (d) 61.3 GHz

Fig. 8 – 2D radiation patterns from CST and HFSS at (a) 28 GHz, (b) 37.8 GHz, (c) 44.8 GHz, (d) 61.3 GHz

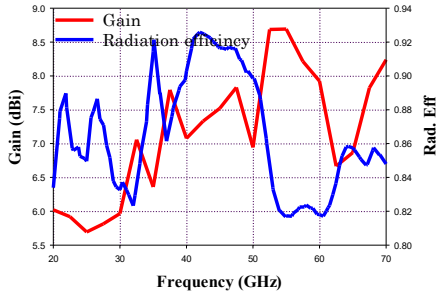

Fig. 9 – Gain and Radiation efficiency over the operational frequency range

4.5 Comparison with Related Work

Table 1 presents a comparative analysis of multi-band microstrip antennas operating in the 20-90 GHz range, summarizing size, frequency bands, bandwidth, gain, and radiation efficiency. The proposed single-element antenna operates at 28, 38, 45, and 60 GHz with bandwidths of 1.6, 2.5, 5, and 15 GHz, offering a competitive balance of bandwidth and gain. While some studies report larger bandwidths (up to 334.2 GHz [16]), the proposed design achieves higher gain than the designs reported in [6] and [17] and wider bandwidth than the antennas presented in [6] and [8], with improved radiation efficiency. Its size, 12 × 12 mm², is more compact relative to all designs listed in Table 1. Overall, the quad-band design achieves low return loss, high gain, and excellent radiation efficiency, validating the design methodology and demonstrating strong potential for 28, 38, 45, and 60 GHz 5G applications.

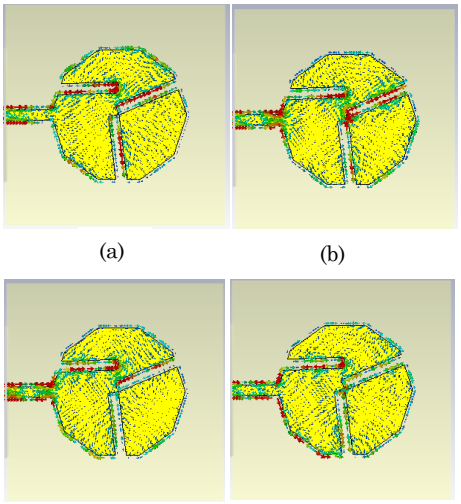

(a) (b)

(c) (d)

Fig. 10 – Surface-current distributions at (a) 28 GHz, (b) 37.8 GHz, (c) 44.8 GHz, (d) 61.3 GHz

5. CONCLUSION

This work presents a decagonal quad-band single-element antenna operating at 28, 38, 45, and 60 GHz. The design was optimized using CST Studio Suite 2022 and validated with Ansys HFSS. The antenna achieves bandwidths of 1.6 GHz (27.2-28.8 GHz**)**, 2.5 GHz (36.9-39.4 GHz), 5 GHz (41.6-46.6 GHz), and 15 GHz (52.7-67.7 GHz), with corresponding gains of 5.9, 7.8, 7.5, and 7.4 dBi at 28, 37.8, 44.8, and 61.3 GHz, respectively. The radiation efficiency ranges from 81.7 % to 93.5 %. Due to the lack of fabrication and measurement facilities, experimental validation was not performed. Future work will focus on antenna fabrication, array and MIMO configurations, and SAR analysis.

Table 1 – The comparison details of the presented antenna with recent published works

Ref	Ant. size (mm²)	*f* (GHz)	BW (GHz)	Gain (dBi)	Rad. Eff. (%)
[6]	15 × 25	38/60	2/3.2 (5.2)	6.5/5.5	89.6/ 79.9
[8]	33 × 27	28/38	1.1/1.3 (2.4)	7.8/9	96/95.5
[13]	24 × 24	28/60	7/20 (27)	9.8/10.8	85/84
[14]	40 × 45	28/38/45	1.2/47.5 (48.7)	10.3 at 40	88 at 42 GHz.
[16]	14 × 16	3.7 to 337.9	3.7 to 337.9 (334.2)	1 to 15	62 to 95
[17]	27 × 29.5	1.91 to 43.5	1.91 to 43.5 (41.59)	2 to 8.2	80 to 90.1
This work	12 × 12	28/38/45 /60	1.6/2.5/5/15 (24.1)	5.9/7.8/7.5 /7.4	81.7- 93.5

REFERENCES

1. M.M. Kamal, S. Yang, S.H. Kiani, M.R. Anjum, M. Alibakhshikenari, Z.A. Arain, A.A. Jamali, Ali Lalbakhsh, E. Limiti, *Electronics* **10** No 12, 1415 (2021).
2. N.N. Tawfeeq, A.H. Sallomi, *e-Prime-Adv. Elect. Eng., Electron. Energy* **10**, 100849 (2024).
3. A. Hilt, *Appl. Sci.* **9** No 23, 5240 (2019).
4. B.A. Esmail, S. Koziel, A. Pietrenko-Dabrowska, D. Isleifson, *Sci. Rep.* **14** No 1, 185 (2024).
5. A.A. Althuwayb, N. Rashid, K. Kaaniche, A.B. Atitallah, O.I. Elhamrawy, V. Sorathiya, S. Lavadiya, *Wireless Netw.* 30 No 1, 495 (2024).
6. M.H. Sharaf, A.I. Zaki, R.K. Hamad, M.M. Omar, *Sensors* **20** No 9, 2541 (2020).
7. S. Tang, Y. Zhang, Z. Han, C.Y. Chiu, R. Murch, *IEEE Antennas Wireless Propag. Lett.* **20** No 12, 2344 (2021).
8. B.O. Icmez, C. Kurnaz, *Appl. Sci.* **15** No 7, 3993 (2025).
9. D. Huang, G. Xu, J. Wu, W. Wang, L. Yang, Z.X. Huang, X.-L. Wu, W.Y. Yin, *IEEE Antennas Wireless Propag. Lett.* **21** No 10, 2025 (2022).
10. H.M. Marzouk, M.I. Ahmed, A.H.A. Shaalan, *Progr. Electromagn. Res. C* **93**, 103 (2019).
11. R.N. Tiwari, O.S. Sai, D. Sharma, M.S. Kumar, P. Singh, P. Kumar, Ch. Sreemanya, S. Rajasekaran, *Res. Eng.* **24**, 103212 (2024).
12. M. Hussain, S.M.R. Jarchavi, S.I. Naqvi, U. Gulzar, S. Khan, M. Alibakhshikenari, I. Huynen, *Electronics* **10** No 21, 2674 (2021).
13. H. El-Hakim, H.A. Mohamed, *J. Infrared Milli. Terahz Waves* **44** No 9, 752 (2023).
14. W. Balani, M. Sarvagya, A. Samasgikar, T. Ali, P. Kumar, *Sensors* **21** No 2, 477 (2021).
15. V. Sharma, N.K. Mishra, A. Agarwal, N.L. Gupta, *Gazi University Journal of Science* **37** No 1, 211 (2024).
16. N. Suguna, S. Revathi, *Appl. Sci.* **13** No 8, 5057 (2023).
17. M. Ayyappan, P. Patel, *IEEE Access* **10**, 76031 (2022).
18. A. Dejen, J. Jayasinghe, M. Ridwan, J. Anguera, *AIMS Electronics and Electrical Engineering* **6** No 1, 1 (2022).
19. S. Ahmad, H. Boubakar, S. Naseer, M.E. Alim, Y.A. Sheikh, A. Ghaffar, A.J.A. Al-Gburi, N.O. Parchin, *Sensors* **22** No 20, 8012 (2022).
20. A.S. Gaid, M.A. Ali, *Iraqi Journal for Electrical & Electronic Engineering*, **19** No 2, 179 (2023).
21. F.M. Abdo, A.S. Gaid, M.M. Saeed, R.A. Saeed, M.A. Alomari, *2025 5th International Conference on Emerging Smart Technologies and Applications (eSmarTA)* (IEEE: 2025).
22. A.S. Gaid, A.A. Sallam, A.M. Aoun, A.A. Saeed, O.Y. Saeed, *International Conference of Reliable Information and Communication Technology*, 728 (Cham: Springer International Publishing: 2020).

Десятикутна чотиридіапазонна щілинна мікросмужкова антена для бездротових мереж 5G

Faez M.B. Abdo[1], Abdul Guddoos S.A. Gaid[1], Mohammad Ahmed Alomari[2], Imran Mohd Ibrahim[3], Mukhtar Ghaleb[4]

[1] *Faculty of Engineering & Information Technology, Taiz University, Taiz, Yemen*
[2] *Faculty of Artificial Intelligence and Cyber Security (FAIX), Universiti Teknikal Malaysia Melaka (UTeM), Melaka, Malaysia*
[3] *Centre for Telecommunication Research and Innovation (CeTRI), Fakulti Teknologi Kejuruteraan Elektronik dan Komputer, Universiti Teknikal Malaysia Melaka (UTeM), Melaka, Malaysia*
[4] *College of Computing and Information Technology, University of Bisha, 67714 Bisha, Saudi Arabia*

Зі швидким розвитком бездротових мереж 5G зростає потреба в компактних, високопродуктивних антенах, здатних працювати в кількох міліметрових діапазонах хвиль. Мікросмужкові патч-антени ідеально підходять для телефонів 5G завдяки своєму низькому профілю та легкості інтеграції. Однак досягнення високого коефіцієнта посилення, широкої пропускної здатності та ефективності в компактному вигляді залишається складним завданням. У цій статті представлена десятикутна чотиридіапазонна мікросмужкова антена, призначена для роботи на частотах 28, 38, 45 та 60 ГГц. Антена, побудована на підкладці Arlon AD 255C (12 × 12 × 0,66 мм^3), має три щілини для покращення узгодження імпедансу та характеристик випромінювання. Результати моделювання показують смуги пропускання 1,6, 2,5, 5 та 15 ГГц з піковим посиленням 5,9, 7,8, 7,5 та 7,4 дБі та ефективністю від 81,7 % до 93,5 %. Запропонована антена має компактний розмір, високий коефіцієнт посилення та багатодіапазонну роботу, що робить її сильним кандидатом для інтеграції в мобільні пристрої 5G наступного покоління.

Ключові слова: Чотиридіапазонна, Щілинна мікросмужкова антена, Компактна антена, Бездротові мережі, 5G.